Peroxisome proliferator-activated receptor-β activation restores the high glucose-induced impairment of insulin signaling in endothelial cells

A.-M. Quintela, R. Jiménez, L Piqueras, M. Gomez-Guzman, J Haro, M.-J. Zarzuelo, Angel Cogolludo, M Sanz, M Toral, M. Romero, et al.

Peroxisome proliferator-activated receptor-β activation restores the high glucose-induced impairment of insulin signaling in endothelial cells.

A M Quintela[1], R Jiménez[1], L Piqueras[2], M Gómez-Guzmán[1], J Haro[3], M J Zarzuelo[1], A Cogolludo [4], M J Sanz[2], M Toral[1], M Romero[1], F Pérez-Vizcaíno[4] and J Duarte[1].

[1]Department of Pharmacology. University of Granada. 18071. Granada. Spain.

[2]Department of Pharmacology, Faculty of Medicine, University of Valencia, Valencia, Spain.

[3]Service of Gynecology, Clinic Hospital of Granada, Granada, Spain.

[4]Department of Pharmacology, School of Medicine, University Complutense of Madrid, IdISSC and Ciber Enfermedades Respiratorias (CIBERES), Madrid, Spain.

Corresponding author: J Duarte. Department of Pharmacology, School of Pharmacy, University of Granada, 18071 Granada, Spain. Tel: (34)-958241791, Fax. (34)-958248264, Email: jmduarte@ugr.es

A M Quintela and R Jiménez: equal contributions as first authors

Running title: PPAR-β and insulin signaling.

This article has been accepted for publication and undergone full peer review but has not been through the copyediting, typesetting, pagination and proofreading process, which may lead to differences between this version and the Version of Record. Please cite this article as doi: 10.1111/bph.12646

SUMMARY

BACKGROUND AND PURPOSE

We analyzed the effects of the peroxisome proliferator-activated receptor β/δ (PPAR-β) agonists, GW0742 and L165041, on the impaired insulin signaling induced by high glucose in human umbilical vein endothelial cells (HUVECs) and aorta and mesenteric arteries from diabetic rats.

EXPERIMENTAL APPROACH

Insulin-stimulated NO production, Akt-Ser473 and eNOS-Ser1177 phosphorylation, and reactive oxygen species (ROS) production were studied in HUVECs incubated in low or high glucose medium. Insulin-stimulated relaxations and protein phosphorylation in vessel from streptozotocin (STZ)-induced diabetic rats were also analyzed.

KEY RESULTS

HUVECs incubated in high glucose medium showed a significant reduction of the insulin-stimulated production of NO. High glucose also reduced insulin-induced Akt-Ser473 and eNOS-Ser1177 phosphorylation, increased IRS-1-Ser636 and ERK1/2-Thr183-Tyr185 phosphorylation and increased ROS production. The coincubation with the PPAR-β agonists GW0742 or L165041 prevented all the effects induced by high glucose. In turn, the effects induced by the agonists were suppressed when HUVEC were also incubated with the PPAR-β antagonist GSK0660, the piruvate dehydrogenase kinase (PDK)-4 inhibitor dichloroacetate or after knockdown of both PPAR-β and PDK4 with siRNA. The ERK1/2 inhibitor PD98059, the ROS scavenger catalase, the inhibitor of complex II thenoyltrifluoroacetone or the uncoupler of oxidative phosphorylation, carbonyl cyanide m-chlorophenylhydrazone also prevented glucose-induced insulin resistance. In STZ diabetic rats, oral GW0742 also improved insulin signaling and the impaired NO-mediated vascular relaxation.

CONCLUSIONS AND IMPLICATIONS

PPAR-β activation *in vitro* and *in vivo* restores the endothelial function, preserving the insulin-Akt-eNOS pathway impaired by high glucose, at least in part, through PDK4 activation.

Keywords: PPAR-β, HUVECs, insulin signaling, reactive oxygen species

Abbreviations: Akt, protein kinase B; AMPK, 5'-AMP-activated protein kinase; CCCP, carbonyl cyanide m-chlorophenylhydrazone; (CPT)-1, carnitine palmitoiltransferase-1; CM-H2DCFDA, 5-(and-6-)chloromethyl-2'-7'-dichlorodihydrofluorescein diacetate; DAF-2, diaminofluorescein-2; DCA, dichloroacetate; eNOS, endothelial nitric oxide synthase; ERK1/2, extracellular signal-regulated kinases1/2; HUVECs, human umbilical vein endothelial cells; IRS, insulin receptor substrate; JNK, c - Jun N-terminal kinases; MAPKs, mitogen-activated protein kinases; mitoQ, mitoquinone; NO, nitric oxide; L-NAME, N^{ω}-Nitro-L-arginine methyl ester; PPARs, peroxisome proliferator-activated receptors; Phe, phenylephrine; PI3K, phosphatidyl-inositol-3 kinase; PDK-4 piruvate dehydrogenase kinase-4; ROS, reactive oxygen species; RT-PCR, Reverse Transcriptase-Polymerase Chain Reaction; STZ, streptozotocin; Mn-SOD, Mn-superoxide dismutase; TTFA, thenoyltrifluoroacetone; TCA, tricarboxylic acid.

Introduction

Insulin resistance is characterized by the failure of insulin to suppress hepatic glucose production or stimulate glucose uptake by peripheral tissues, causing hyperglycemia, hyperinsulinemia and dyslipidemia (Saltiel *et al.*, 2001; Taguchi and White, 2008; White, 2003). It is clinically important because it is closely associated with several diseases including type 2 diabetes, hypertension, dyslipidemia and abnormalities in blood coagulation and fibrinolysis. One of the key vascular actions of insulin is to stimulate the production of the potent vasodilator nitric oxide (NO) from the endothelium (Vincent *et al*., 2003) and, hence, insulin-resistance is characterized by reduced insulin-induced NO release which may contribute to increased risk of vascular disease (Boden, 2011). The impaired insulin signaling in endothelial cells causes attenuation of insulin-induced capillary recruitment and insulin delivery, which, in turn, leads to a further reduction in glucose uptake by skeletal muscle (Kubota *et al*., 2011).

The peroxisome proliferator-activated receptors (PPARs) are members of the nuclear hormone receptor superfamily. PPARs comprise three related receptors: PPAR-α, PPAR-β/δ (PPAR-β), and PPAR-γ. PPARs were initially believed to regulate genes involved only in lipid and glucose metabolism (Desvergne and Wahli, 1999; Lee *et al*., 2003). PPAR-α is highly expressed in liver, where it controls peroxisomal and mitochondrial fatty acid catabolism, whereas PPAR-γ is abundant in adipose tissues, functioning as a key transcriptional factor for adipogenesis. The PPAR-α activators, such as the fibrates, are used for the treatment of hyperlipidemia, whereas PPAR-γ agonists, such as the thiazolidinediones, are used to treat type 2 diabetes because they improve insulin action and decrease intracellular triglyceride accumulation in both liver and skeletal muscle (Miyazaki *et al*., 2002; Tonelli *et al*., 2004). PPAR-β is expressed in most metabolically active tissues, controlling many genes involved in fatty acid

metabolism and glucose homeostasis (Braissant *et al*., 1996; Wang *et al*., 2003). PPAR-β has been shown to increase fat oxidation and reduce lipid accumulation in adipose tissue and in other tissues (Reilly and Lee, 2008). Furthermore, studies in rodents have shown that activation of PPAR-β reduces body weight, increases metabolic rate and improves insulin sensitivity, through increased skeletal muscle fatty acid oxidation (Wang *et al*., 2003). In diabetic db/db mice, a long-term PPAR-β activation improves insulin sensitivity and islet function along with an improved lipid profile, suggesting that PPAR-β activation might be a target for the treatment of type 2 diabetes (Winzell *et al*., 2010).

Several lines of evidence indicate that activation of PPAR-β enhances insulin sensitivity in adipocytes and skeletal muscle cells improving the glucose metabolism and the lipid profile (Wang *et al*., 2003, Leibowitz *et al*., 2000; Oliver Jr *et al*., 2001; Tanaka *et al*., 2003; Krämer *et al*., 2005; Fritz *et al*., 2006; Coll *et al*., 2010; Serrano-Marco *et al*., 2011). There are also studies reporting the opposite or no effects of PPAR-β stimulation in different in vitro models (Dimopoulos *et al*., 2007; Terada *et al*., 2006; Brunmair *et al*., 2006; Cresser *et al*., 2010). However, if PPAR-β activation affects insulin signaling in endothelial cells are unknown. Therefore, we examined the possible protective effects of the PPAR-β agonists on impaired insulin signaling induced *in vitro* by high glucose in cultured primary human umbilical vein endothelial cells (HUVECs), and *in vivo* in arterial vessel from diabetic rats.

Methods

Cell cultures

Endothelial cells were isolated from human umbilical cord veins using a previously reported method with several modifications (Jiménez *et al*., 2010). The cells were cultured (Medium 199 + 20% fetal bovine serum + Penicillin/Streptomycin 2mmol/L + Amphotericin B 2 mmol/L + Glutamine 2 mmol/L + HEPES 10 mmol/L + endothelial cell growth supplement 30 μg/mL + Heparin 100 mg/mL) under 5% CO_2 at 37°C. HUVECs were incubated with the PPAR-β agonists, GW0742 or L165041 (1 or 10 μmol/L) or the PPAR-α agonist, clofibrate (1μmol/L), or the PPAR-γ agonist, ciglitazone (1μmol/L), or the extracellular signal-regulated kinases (ERK)1/2 inhibitor, PD98059 (10 μmol/L), or the c-Jun N-terminal kinases (JNK) inhibitor, SP600125 (25 μmol/L), during 24 hours in low (5 mmol/L) or high glucose (30 mmol/L) medium. In some experiments, cells were coincubated with the PPAR-β antagonist GSK0660 (1 μmol/L) 1 hour prior the addition of each PPAR-β agonist. Cells were then used to measure NO production by diaminofluorescein-2 (DAF-2) fluorescence or to analyze protein expression or phosphorylation by Western blot under basal conditions or after the exposure to insulin (500 nmol/L).

Transfection of PPAR-β and PDK4 siRNAs

Confluent HUVECs were transfected with control or PPAR-β- or PDK4-specific siRNA (pooled, validated siRNA from Dharmacon, Lafayette, CO, USA) using Lipofectamine RNAiMAX (Invitrogen) for 48 h, essentially as described previously (Piqueras *et al*., 2009).

Quantification of NO released by DAF-2

Quantification of NO released by HUVECs was performed using the NO-sensitive fluorescent probe DAF-2 as described previously (Jiménez *et al*., 2010). Briefly, cells

were incubated as mentioned above during 24 hours. After this period, cells were washed with PBS and then were pre-incubated with L-arginine (100 μmol/L in PBS, 5 min, 37ºC). Subsequently, DAF-2 (0.1 μmol/L) was incubated for 2 min and then either insulin (500 nmol/L) or the calcium ionophore calimycin (A23187, 1 μmol/L) were added for 30 min and cells were incubated in the dark at 37ºC. Then the fluorescence was measured using a spectrofluorimeter (Fluorostart, BMG Labtechnologies, Offenburg, Germany). The auto-fluorescence was subtracted from each value.

Protein expression and phosphorylation

Cells were incubated as mentioned above for 12 hours for ERK1/2 analysis or 24 hours for the rest of proteins or submitted to the siRNA procedure for 48 h. Then western blotting was performed as described previously (Jiménez *et al*., 2010).

Reverse transcriptase-polymerase chain reaction (RT-PCR) analysis

For Reverse Transcriptase-Polymerase Chain Reaction (RT-PCR) analysis, total RNA was extracted from HUVECs by homogenization and converted to cDNA by standard methods. Polymerase chain reaction was performed with a Techne Techgene thermocycler (Techne, Cambridge, UK). A quantitative real-time RT-PCR technique was used to analyze mRNA expression (Zarzuelo *et al*., 2011). The sequences of the primers used for amplification of HUVECs samples are: PPAR-β, sense CATTGAGCCCAAGTTCGAGT, and antisense GGTTGACCTGCAGATGGAAT; piruvate dehydrogenase kinase (PDK)-4, sense AGGTCGAGCTGTTCTCCCGCT and antisense GCGGTCAGGCAGGATGTCAAT, Mn-superoxide dismutase (SOD) sense GCCGTAGCTTCTCCTTAAA and antisense GCTACGTGAACAACCTGAA and for rat aorta samples, sense CCTAAGGGTGGTGGAGAACC and antisense

CTGTGGTTCCTTGCAGTGG. Relative quantification of these different transcripts was determined with the ΔΔCt method using GAPDH and β-actin as endogenous control, respectively, and normalized to control group.

Measurement of intracellular reactive oxygen species (ROS) concentrations

The fluorescent probe 5-(and-6-)chloromethyl-2'-7'-dichlorodihydrofluorescein diacetate (CM-H2DCFDA) was used to determine the intracellular generation of ROS in endothelial cells. Confluent HUVEC in 96-well plates were grown in 5 or 30 mmol/L glucose in the presence or absence of either L165041 (1μmol/L), or the inhibitor of complex I rotenone (5 μmol/L), or the inhibitor of complex II, thenoyltrifluoroacetone (TTFA 10 μmol/L), or the uncoupler of oxidative phosphorylation, carbonyl cyanide m-chlorophenylhydrazone (CCCP, 0.5 μmol/L) for 24 hours. Inhibitors (GSK0660 1μmol/L, or dichloroacetate (DCA) 10 μmol/L, or the mitochondrial antioxidant mitoquinone (mitoQ, generously given by Dr. MP Murphy, Medical Research Council Mitochondrial Biology Unit, Cambridge, UK, 0.1 μmol/L) were added 30 min for GSK0660 and DCA, and 60 min for mitoQ before the incubation with L165041. Thereafter, the cells were incubated with 5 μmol/L CM-H2DCFDA for 30 min at 37 ºC. The fluorescent intensity was measured using a spectrofluorimeter (Fluorostart, BMG Labtechnologies, Offenburg, Germany).

Animals and experimental groups

The experimental protocol followed the European Union guidelines for animal care and protection. Male Wistar rats were randomized to 3 experimental groups: untreated control group (vehicle, 1 mL of 1% methylcellulosa), untreated diabetic (vehicle), and GW0742-treated diabetic group (5 mg kg^{-1} per day, mixed in 1 mL of 1%

methylcellulose, by oral gavage). Diabetic rats received a single injection via tail vein of streptozotocin (STZ, 50 mg kg^{-1} dissolved in a citrate buffer at pH, 4.5). Rats with blood glucose levels of 200 mg dL^{-1} or above and polyuria were considered to be diabetic. GW0742 treatment was started 4 days after STZ injection, and the treatment continued for 3 days.

Vascular reactivity studies

Descending thoracic aortic rings (3 mm) and the third branch of the mesenteric artery (1.7-2 mm) were dissected from animals and were mounted in organ chambers and in a wire myograph, respectively. After equilibration, vessels were contracted by phenylephrine (Phe, 1 μmol/L) and concentration-relaxation response curves were performed by cumulative addition of insulin in the absence or presence (added 1 h before Phe) of the PDK-4 inhibitor (DCA, 10 μmol/L), or the mitochondrial antioxidant mitoQ (0.1 μmol/L), or the eNOS inhibitor N^{ω}-Nitro-L-arginine methyl ester (L-NAME, 100 μmol/L, 15 min before Phe). The concentration-relaxation response curves to sodium nitroprusside were performed in the dark in aortic rings without endothelium pre-contracted by 1 μmol/L Phe.

In order to analyse endothelial NO synthase (eNOS) and protein kinase B (Akt) phosphorylation, some aortic rings were incubated for 15 min with insulin (100 nmol/L) in Krebs solution. Other rings were used to measure ERK1/2, AMPK, and IRS-1 phosphorylation, and PPAR-β protein expression by western blot (Jiménez *et al.*, 2010).

Statistical analyses

Values are expressed as mean ± SEM. Statistical comparisons were performed using a Student's *t* tests or one-way ANOVA with Bonferroni's procedure for post hoc analysis. Values of $p<0.05$ were considered significant.

Results

High glucose inhibits insulin-stimulated NO production and protein kinase B (Akt) and endothelial NO synthase (eNOS) phosphorylation

Exposure of HUVECs to insulin (0.1-500 nmol/L) increased, in a concentration-dependent manner, the DAF-2 fluorescence intensity compared to non-stimulated cells (Suppl. Figure 1A, Figure 1A). The fluorescent signal was abolished by the eNOS inhibitor N^{ω}-Nitro-L-arginine methyl ester (L-NAME, 100 μmol/L, Suppl. Figure 2A). Moreover, the phosphatidyl-inositol-3 kinase (PI3K) inhibitor LY-294002 (10 μmol/L) suppressed the insulin-increased DAF-2 fluorescence (Suppl. Figure 2A). Incubation in high glucose medium (10, 15, or 30 mmol/L, for 24 h) reduced significantly both basal and insulin (500 nmol/L)-dependent NO production as compared to cells exposed to low glucose (Suppl. Figure 1B, Figure 1A). In order to study if PPAR-β activation was able to prevent the impairment of insulin signaling in extremely high glucose levels we performed the rest of experiments using 30 mmol/L. To investigate whether this inhibitory effect of high glucose was restricted to insulin-stimulated NO synthesis, we next examined the effect of high glucose on NO production stimulated by the calcium ionophore A23187 (Figure 1B). A23187 rapidly stimulated NO synthesis in HUVECs and there was no significant difference in the response of cells incubated at low or high glucose concentration. A23187-dependent NO production was abolished by eNOS inhibitor L-NAME or the intracellular Ca^{2+} quelator BAPTA-AM (10 μmol/L) (Suppl.

Figure 2B). Insulin induced an increase in Akt (Figure 1C) and eNOS (Figure 1D) phosphorylation. Moreover, exposure of HUVECs to high glucose caused a reduction in the phosphorylation of both basal and insulin-stimulated Akt (Figure 1C) and eNOS (Figure 1D) phosphorylation.

PPAR-β activation restores the high glucose-induced impairment of the insulin-Akt-eNOS pathway

When HUVECs were incubated in low glucose medium for 24 hours, coincubation with PPAR-β agonists, GW0742 or L165041 (1 or 10 μmol/L), did not change NO production (Figure 2A, 2B) stimulated by insulin. However, both PPAR-β agonists increased insulin-mediated NO production in HUVECs exposed to high glucose medium (Figure 2C, 2D). These effects were suppressed when HUVEC were co-incubated with the PPAR-β antagonist GSK0660 (1 μmol/L). Both PPAR-β agonists also increased insulin-stimulated Akt (Figure 2E) and eNOS (Figure 2F) phosphorylation and again these effects were prevented by GSK0660 (1 μmol/L).

To confirm these observations further, in another set of experiments, HUVECs were treated with control or pooled, validated PPAR-β siRNA. Forty-eight hours post-transfection with PPAR-β-specific siRNA, HUVECs showed a > 80% decrease in mRNA PPAR-β (Figure 3A) and > 85% protein (Figure 3B) relative to control siRNA treated cells. PPAR-β-specific but not control siRNA abolished the increase in insulin-stimulated NO production induced by both PPAR-β ligands in cells incubated in high glucose medium (Figure 3C).

To determine whether this protective effect on insulin-stimulated NO production is selective for PPAR-β activation or it is shared by other PPARs, we next examined the effects of a selective PPAR-α, clofibrate, or a PPAR-γ ligand, ciglitazone. The

incubation with either agent also prevented the decrease in insulin-stimulated NO synthesis induced by high glucose (Suppl. Figure 3).

Role of 5'-AMP-activated protein kinase (AMPK) and mitogen-activated protein kinases (MAPKs)

To determine whether AMPK is involved in the protective effects of PPAR-β agonists, we examined the effect of AMPK inhibitor, compound C, on insulin stimulated NO-production (Suppl. Figure 4A) and the effects of PPAR-β agonists on Thr-172 AMPK phosphorylation (Suppl. Figure 4B). AMPK inhibition with previous incubation (1 hour before NO determination) with compound C did not modify the increased insulin-stimulated NO production induced by both GW0742 and L165041 (10 μmol/L) in HUVECs exposed to high glucose (Suppl. Figure 4A). Moreover, AMPK phosphorylation was not altered by high glucose medium and neither GW0742 nor L165041 induced any change in AMPK phosphorylation (Suppl. Figure 4B).

To explore the role of MAPKs we analyzed the effects of the ERK1/2 inhibitor, PD98059 (10 μmol/L), or the JNK inhibitor, SP600125 (25 μmol/L) in insulin-stimulated NO production in HUVECs incubated in high-glucose medium (Suppl. Figure 4C). ERK1/2 inhibition restored the insulin-stimulated NO synthesis while the JNK inhibitor was without effect. Moreover, high glucose induced ERK1/2 phosphorylation at 12 h was suppressed by coincubation with either 10 μmol/L GW0742 or 10 μmol/L L165041 (Suppl. Figure 4D).

Role of PPAR-β target genes, carnitine palmitoiltransferase (CPT)-1 and piruvate dehydrogenase kinase (PDK)4

We analyzed the role of the PPAR-β target genes CPT-1 and PDK4 in the effects of the PPAR-β agonists by measuring insulin-stimulated NO production in high glucose medium in the presence of etomoxir, an irreversible inhibitor of CPT-1, or DCA, an inhibitor of PDK4. In these experimental conditions, DCA abolished the increased NO production induced by both GW0742 and L165041 while etomoxir was without effect (Figure 4A). PDK4 mRNA levels were also increased in a concentration-dependent manner by either GW0742 (Figure 4B) or L165041 (Figure 4C), in HUVECs incubated in low and high-glucose conditions. This effect was abolished by coincubation with the PPAR-β antagonist GSK0660. To confirm these observations further, in another set of experiments, HUVECs were treated with control or pooled, validated PDK4 siRNA. Forty-eight hours post-transfection with PDK4-specific siRNA, HUVECs showed a > 70 % decrease in PDK4 protein Figure 4D) relative to control siRNA treated cells. PDK4-specific but not control siRNA abolished the increase in insulin-stimulated NO production induced by both PPAR-β ligands in cells incubated in high glucose medium (Figure 4D).

Effects of PPAR-β agonists on intracellular ROS production

To test whether the protective effects of PPAR-β agonist L165041 might be related to inhibition of ROS we measured intracellular ROS in HUVECs incubated in low and high glucose medium. Compared to baseline conditions (5 mmol/L glucose), incubation with 30 mmol/L glucose increased ROS production (Figure 5A). Rotenone did not reduce this increased ROS production, whereas TTFA, CCCP, and mitoQ completely prevented the effect of high glucose. Incubation with L165041 (1 μmol/L) also abolished high glucose-induced intracellular ROS production. Coincubation of this PPAR-β agonist with either GSK0660 or DCA suppressed the inhibition of ROS

production induced by L165041 in high glucose medium. Moreover, both PPAR-β- (Figure 5B) and PDK4-specific (Figure 5C) but not control siRNA abolished the inhibitory effect of L165041 in high glucose-induced mitochondrial ROS overproduction. In addition, Mn-SOD mRNA levels were increased in HUVECs incubated with L165041 and GW0742 in both low and high glucose conditions (Figure 5D).

To test if mitochondrial ROS are involved in ERK1/2 activation we analyzed ERK1/2 phosphorylation in HUVECs incubated in the presence of TTFA or catalase. Both agents suppressed the increased ERK1/2 phosphorylation induced by high glucose (Figure 5E).

Effects of PPAR-β agonists on insulin receptor substrate (IRS) phosphorylation

High glucose increased both Ser-636-IRS-1 (Figure 6A) and Ser-270-IRS1/2 (Figure 6B) phosphorylation in HUVEC. This effect was abolished by the presence of PPAR-β agonists GW0742 or L165041 (Figure 6). Coincubation with the PPAR-β antagonist GSK0660 restored the level of phosphorylation induced by high glucose. Interestingly, the presence of the ERK1/2 inhibitor, PD98059, also suppressed the increase in IRS-1/2 phosphorylation induced by high glucose.

GW0742 treatment in vivo improves insulin-induced vasodilatation in STZ-induced diabetic rats in a PDK4-dependent manner

GW0742 treatment did not modify the increase in plasma glucose (Figure 7A) induced by STZ injection but increased the expression of aortic PDK4 and MnSOD (Figure 7B). ERK1/2 and Ser-636-IRS-1 phosphorylation was increased in diabetic rats, and restored at control values after GW0742 treatment (Suppl. Figure 5). No significant changes

were observed among groups in AMPK phosphorylation. However, aortic PPAR-β protein expression was increased in STZ group and significantly increased by GW0742 treatment (Suppl. Figure 5). Akt and eNOS phosphorylation induced by insulin were decreased in aorta from STZ rats compared to controls and these changes were prevented by GW0742 (Figure 7C). In the aorta (Figure 7D) and the mesenteric resistance arteries (Figure 7E) isolated from diabetic rats the relaxations induced by insulin were reduced. In vessels from diabetic rats treated with GW0742 the relaxations induced by insulin were preserved. Treatment of the arteries *in vitro* with mitoQ also restored the relaxation. The improvement of insulin relaxation induced by GW0742 was suppressed when the vessels were incubated with the PDK4 inhibitor DCA. These relaxant responses to insulin in aortic rings were suppressed by the NOS inhibitor L-NAME (100 μmol/L) (suppl. Figure 6A). Endothelium-independent relaxations to nitroprusside were similar among groups (suppl. Figure 6B).

Discussion and conclusions

Several lines of evidence indicate that activation of PPAR-β enhances insulin sensitivity in adipocytes and skeletal muscle cells (Wang *et al*., 2003, Leibowitz *et al*., 2000; Oliver Jr *et al*., 2001; Tanaka *et al*., 2003; Krämer *et al*., 2005; Fritz *et al*., 2006; Coll *et al*., 2010; Serrano-Marco *et al*., 2011). Herein, we report that in human endothelial cells and rat arteries activation of PPAR-β via PDK4 upregulation prevented the high glucose-induced impairment of insulin-stimulated NO production and relaxation. This protective effect seems to be related to the inhibition of mitochondrial ROS production and ERK1/2 activation.

Insulin receptor activation (Figure 8) results in phosphorylation of multiple tyrosine residues of IRS-1, which then activates PI3K, leading to phosphorylation and

activation of protein kinase (PDK-1). PDK-1, in turn, phosphorylates and activates Akt, which finally phosphorylates eNOS at the activator site Ser1177 increasing eNOS activity and NO production (Vincent *et al*., 2003). In endothelial cells exposed to high glucose, the insulin-stimulated NO production is impaired (Schnyder *et al*., 2002; Salt *et al*., 2003; Kim *et al*., 2005), but the mechanisms are not fully characterized. It has been reported that high glucose inhibits basal eNOS expression, activity, and NO production in cultured endothelial cells (Ding *et al*., 2000; Du *et al*., 2001). This has been related to increased ROS production which may decrease NO via different mechanisms (Muniyappa *et al*., 2007): 1) Direct decrease of NO bioavailability (e.g. the direct reaction of NO with superoxide), 2) Reduction of cellular tetrahydrobiopterin levels promoting eNOS uncoupling, 3) Formation of advanced glycation end-products, which inhibit the PI3K/Akt/eNOS pathway and accelerate eNOS mRNA degradation (Wallis *et al*., 2005; Xu *et al*., 2003; Goldin *et al*., 2006), 4) O-linked N-acetylglucosaminylation of eNOS at the Akt phosphorylation site at Ser1179 resulting in impaired eNOS activity (Du *et al*., 2001), and 5) Stimulation of serine-636 phosphorylation of IRS-1 which reduces the binding of p85 regulatory subunit of PI3K to IRS-1 and promoting insulin resistance (Esposito *et al*., 2001). MAPKs, such as ERK1/2 and JNK, are stress-activated protein kinases, which may interfere with insulin signaling by phosphorylation of IRS-1 at serine-636 (Rains and Jain, 2011). In our experimental conditions high glucose reduced both insulin-dependent NO production and (Ser473)-Akt and (Ser1177)-eNOS phosphorylation as compared to cells exposed to low glucose. This effect was restricted to insulin-stimulated eNOS activation because the A23187-induced NO production was unaffected by high glucose. Our results are in agreement with the hypothesis involving the increase in mitochondrial ROS production, the subsequent ERK1/2 phosphorylation and the IRS-1 (Ser636) and IRS-1/2 (Ser270)

phosphorylation in the impairment of insulin-stimulated NO production. This is further supported by several findings. First, TTFA, an inhibitor of complex II of mitochondrial electron transport chain, and CCCP, an uncoupler of oxidative phosphorylation, and the mitochondrial antioxidant mitoQ inhibited high glucose-induced increase in ROS production (current results, and Nishikawa *et al*., 2000) and increased insulin-stimulated NO production. Second, in agreement with previous results (Chen *et al*., 2007), high glucose increased ERK1/2 phosphorylation in HUVECs and in aorta from STZ group, which was inhibited by TTFA and by the H_2O_2 scavenger catalase, suggesting that ERK1/2 is activated by ROS. ERK1/2 inhibition by PD98059 also increased insulin-stimulated NO production in HUVECs incubated in high-glucose medium, being without effect the JNK inhibitor, SP600125. Third, serine phosphorylation of IRS-1/2 was stimulated by high glucose in HUVECs and in aorta from diabetic rats, and inhibited by the ERK1/2 inhibitor PD98059.

In agreement with Quintela *et al.*, (2012) the protein expression of PPAR-β increased in the aorta from diabetic as compared with control rats, and was up-regulated by GW0742 treatment. Activation of PPAR-β prevented the high glucose-induced impairment of the insulin signal to produce NO and arterial relaxation. This is supported by several data. First, PPAR-β agonists, GW0742 and L165041, increased the NO production stimulated by insulin in high glucose cultured cells, being without effect in cells incubated in low glucose. This improvement in endothelial function was accompanied by increased Akt and eNOS phosphorylation. Second, *in vivo* GW0742 treatment also increased Akt and eNOS phosphorylation and improved NO-dependent insulin relaxation in aorta and mesenteric arteries from STZ rats. Similar results showing that PPAR-β activation protects endothelial function and improves insulin-induced relaxation in diabetic and obese mice have been previously described (Tian *et*

al., 2012). However, these authors did not establish a clear link between the improvement of insulin relaxation and changes in insulin-stimulated PI3K/Akt/eNOS pathways. Our results are consistent with the mechanism of the physiological actions of insulin on the vascular endothelium, which is predominantly mediated via the IRS/PI3K/Akt pathway (as described above). Third, the activation of PPAR-β by the agonists in these experiments is demonstrated by the upregulation of PDK4, a canonical PPAR-β target gene. Both functional and expressional effects induced by both agonists were suppressed when HUVEC were co-incubated with the PPAR-β antagonist GSK0660. Moreover, PPAR-β-specific siRNA also abolished the protective effects of PPAR-β agonists in insulin-stimulated NO production. This protective effect on NO production was not restricted to PPAR-β activation, since a similar effect was also evoked by either PPAR-α agonist clofibrate or PPAR-γ ciglitazone.

Several mechanisms have been involved on the protective effects of PPAR-β agonists on insulin resistance, such as activation of AMPK (Barroso *et al*., 2011), ERK1/2 inhibition (Rodríguez-Calvo *et al*., 2008), and CPT-1 activation (Coll *et al*., 2010). AMPK is a metabolic sensor that detects low ATP levels and in turn increasing oxidative metabolism (Reznick *et al*., 2006) by reducing the levels of malonyl-CoA, which inhibits CPT-1 activity. High glucose increases ATP synthesis by the mitochondria, leading to AMPK inhibition, at least, in rat mesangial cells (Lv *et al*., 2012), which might induce a reduction in eNOS Ser-1177 phosphorylation and bioactivity (Thors *et al*., 2008). However, in our experimental conditions no changes in AMPK phosphorylation/activation were found. The PPAR-β ligand GW5015116 increased the AMP to ATP ratio in liver (Barroso *et al*., 2011) and skeletal muscle cells (Krämer *et al*., 2007) increasing AMPK phosphorylation. Our present data in HUVECs, in hyperglycemic conditions, are in disagreement with these previous evidences, since

no significant increase in AMPK phosphorylation were found after either GW0742 or L165041 treatment, and also no change in the effects of both PPAR-β agonists improving insulin-stimulated NO production was detected after AMPK inhibition by compound C. Moreover, AMPK phosphorylation was unchanged in aorta from STZ as compared to control rats.

As described above ERK1/2 activation seems to be involved in the impaired insulin signaling induced by high glucose. Protective effects of PPAR-β agonists in lipopolysaccharide-induced cytokine production in adipocytes (Rodríguez-Calvo *et al*., 2008) and PDGF-induced rat vascular smooth muscle proliferation (Lim *et al*., 2009) seem to be related to prevention of ERK1/2 phosphorylation. In our experiments, both PPAR-β agonists reduced ERK1/2 activation induced by high glucose in HUVECs, and also prevented the increased serine phosphorylation of IRS-1/2. This data in endothelial cells confirms that PPAR-β regulates phospho-ERK1/2 levels in several tissues. In fact, similar results were found in aorta from diabetic rats after GW0742 treatment. However, the molecular mechanisms by which PPAR-β controls ERK1/2 activation are unclear. Inhibitory cross talk between ERK1/2 and AMPK has been reported (Du *et al*., 2008), which can be ruled out in our experiment since both PPAR-β agonists did not increased AMPK activity. ERK1/2 is a stress-sensitive serine/threonin protein kinase. In our experiments, ERK1/2 activation was inhibited by TTFA and catalase, suggesting a role for mitochondrial ROS as a cellular stimuli for ERK1/2 activation.

The glucose metabolism begins with glycolysis generating NADH and pyruvate. Pyruvate can be transported into the mitochondria, where it is oxidized by the pyruvate dehydrogenase complex yielding acetyl-CoA, which enters the tricarboxylic acid (TCA) cycle to produce NADH and $FADH_2$. Mitochondrial NADH and $FADH_2$ lead to ATP production through oxidative phosphorylation by the electron transport chain (ETC).

Inhibition of pyruvate transport into the mitochondria inhibited hyperglycemia-induced ROS production, indicating that the mitochondrial TCA cycle-ETC complex is the major source for ROS generation (Nishikawa *et al*., 2000). PDK-4 is a key enzyme that mediates the shift from glycolytic to fatty acid oxidative metabolism via pyruvate dehydrogenase phosphorylation and subsequent inactivation (Patel and Korotchkina, 2006). PPAR-β is a key regulator of PDK genes, in particular the PDK4 gene (Degenhardt *et al*., 2007). In fact, we found that both PPAR-β agonists increased in a concentration-dependent manner the mRNA levels of PDK4 in HUVECs in either low or high glucose medium, and this effect was inhibited by blocking PPAR-β with GSK0660. Furthermore, in vivo GW0742 treatment also increased PDK4 expression in aorta from STZ rats. Moreover, inhibition of PDK4 by both DCA or by PDK4-specific siRNA suppressed the inhibitory effects of L165041 in high glucose-induced mitochondrial ROS overproduction and also inhibited the increased insulin-mediated NO production induced by PPAR-β activation in high glucose medium. In addition, DCA also suppressed the improvement of insulin relaxation induced by GW0742 in aorta and small mesenteric arteries from diabetic rats.

Overexpression of MnSOD completely prevented the effect of hyperglycemia (Du *et al*., 2001). We found that mRNA levels of MnSOD in high glucose conditions *in vitro* and *in vivo* were reduced as compared to low glucose. Interestingly, activation of PPAR-β increased MnSOD expression in vascular cells, which would collaborate to reduce mitochondrial ROS production.

Taking into account that insulin signaling in endothelial cells seems to play a pivotal role in the regulation of glucose uptake by skeletal muscle (Kubota *et al*., 2011), activation of PPAR-β, which improves endothelial insulin signaling inducing NO-dependent relaxation, may serve as a therapeutic strategy for ameliorating skeletal

muscle insulin resistance. However, this improvement of insulin signaling found in aorta from STZ rats treated by GW0742 was unable to lower blood glucose, possibly as a result of insufficient plasma insulin levels derived from beta-cells destruction.

In summary, we report that the PPAR-β ligands, both *in vitro* and *in vivo*, through upregulation of PDK4, prevent the high glucose-induced impairment of the PI3K-Akt-eNOS pathway, leading to increase NO production stimulated by insulin in HUVECs and in rat aorta and mesenteric arteries (Figure 8). PDK4 and MnSOD overexpression normalizes mitochondrial ROS production and ERK1/2 activity thereby restoring insulin-stimulated IRS-Akt-eNOS signaling.

Acknowledgments

This work was supported by Grants from Comisión Interministerial de Ciencia y Tecnología (SAF2011-28150, SAF2010-22066-C02-01 and -02) and by the Ministerio de Ciencia e Innovación, Instituto de Salud Carlos III (Red HERACLES RD06/0009), Spain. María José Zarzuelo and Ana María Quintela are holders of studentships from Spanish Ministry of Science and Education.

Conflicts of interest

None.

References

Barroso E, Rodríguez-Calvo R, Serrano-Marco L, Astudillo AM, Balsinde J, Palomer X *et al.* (2011). The PPAR-β activator GW501516 prevents the down-regulation of AMPK

caused by a high-fat diet in liver and amplifies the PGC-1α-Lipin 1-PPARα pathway leading to increased fatty acid oxidation. Endocrinology 152: 1848-1859.

Boden G (2011). Obesity, insulin resistance and free fatty acids. Curr Opin Endocrinol Diabetes Obes 18: 139-143.

Braissant O, Foufelle F, Scotto C, Dauça M, Wahli W (1996). Differential expression of peroxisome proliferator-activated receptors (PPARs): tissue distribution of PPAR-alpha, -beta, and -gamma in the adult rat. Endocrinology 137: 354-366.

Brunmair B, Staniek K, Dörig J, Szöcs Z, Stadlbauer K, Marian V *et al*. (2006). Activation of PPAR-delta in isolated rat skeletal muscle switches fuel preference from glucose to fatty acids. Diabetologia 49: 2713-2722.

Chen YH, Guh JY, Chuang TD, Chen HC, Chiou SJ, Huang JS *et al*. (2007). High glucose decreases endothelial cell proliferation via the extracellular signal regulated kinase/p15(INK4b) pathway. Arch Biochem Biophys 465: 164-171.

Coll T, Alvarez-Guardia D, Barroso E, Gómez-Foix AM, Palomer X, Laguna JC *et al*. (2010). Activation of peroxisome proliferator-activated receptor-{delta} by GW501516 prevents fatty acid-induced nuclear factor-{kappa}B activation and insulin resistance in skeletal muscle cells. Endocrinology 151: 1560-1569.

Cresser J, Bonen A, Chabowski A, Stefanyk LE, Gulli R, Ritchie I *et al*. (2010). Oral administration of a PPAR-delta agonist to rodents worsens, not improves, maximal

insulin-stimulated glucose transport in skeletal muscle of different fibers. Am J Physiol Regul Integr Comp Physiol 299: R470-R479.

Degenhardt T, Saramäki A, Malinen M, Rieck M, Väisänen S, Huotari A *et al.* (2007). Three members of the human pyruvate dehydrogenase kinase gene family are direct targets of the peroxisome proliferator-activated receptor beta/delta. J Mol Biol 372: 341-355.

Desvergne B, Wahli W (1999). Peroxisome proliferator-activated receptors: nuclear control of metabolism. Endocr Rev 20: 649-688.

Dimopoulos N, Watson M, Green C, Hundal HS (2007). The PPARdelta agonist, GW501516, promotes fatty acid oxidation but has no direct effect on glucose utilisation or insulin sensitivity in rat L6 skeletal muscle cells. FEBS Lett. 581: 4743-4748.

Ding Y, Vaziri ND, Coulson R, Kamanna VS, Roh DD (2000). Effects of simulated hyperglycemia, insulin, and glucagon on endothelial nitric oxide synthase expression. Am J Physiol Endocrinol Metab 279: E11-E17.

Du J, Guan T, Zhang H, Xia Y, Liu F, Zhang Y (2008). Inhibitory crosstalk between ERK and AMPK in the growth and proliferation of cardiac fibroblasts. Biochem Biophys Res Commun 368: 402-407.

Du XL, Edelstein D, Dimmeler S, Ju Q, Sui C, Brownlee M (2001). Hyperglycemia inhibits endothelial nitric oxide synthase activity by posttranslational modification at the Akt site. J Clin Invest 108: 1341-1348.

Esposito DL, Li Y, Cama A, Quon MJ (2001). Tyr(612) and Tyr(632) in human insulin receptor substrate-1 are important for full activation of insulin-stimulated phosphatidylinositol 3-kinase activity and translocation of GLUT4 in adipose cells. Endocrinology 142: 2833-2840.

Fritz T, Krämer DK, Karlsson HK, Galuska D, Engfeldt P, Zierath JR *et al.* (2006). Low-intensity exercise increases skeletal muscle protein expression of PPARδ and UCP3 in type 2 diabetic patients. Diabetes Metab Res Rev 22: 492-498.

Goldin A, Beckman JA, Schmidt AM, Creager MA (2006). Advanced glycation end products: sparking the development of diabetic vascular injury. Circulation 114: 597-605.

Jiménez R, Sánchez M, Zarzuelo MJ, Romero M, Quintela AM, López-Sepúlveda R *et al.* (2010). Endothelium-dependent vasodilator effects of peroxisome proliferator-activated receptor beta agonists via the phosphatidyl-inositol-3 kinase-Akt pathway. J Pharmacol Exp Ther 332: 554-561.

Kim F, Tysseling KA, Rice J, Gallis B, Haji L, Giachelli CM *et al*. (2005). Activation of IKKbeta by glucose is necessary and sufficient to impair insulin signaling and nitric oxide production in endothelial cells. J Mol Cell Cardiol 39: 327-334.

Krämer DK, Al-Khalili L, Guigas B, Leng Y, Garcia-Roves PM, Krook A (2007). Role of AMP kinase and PPARdelta in the regulation of lipid and glucose metabolism in human skeletal muscle. J Biol Chem 282: 19313-19320.

Krämer DK, Al-Khalili L, Perrini S, Skogsberg J, Wretenberg P, Kannisto K et al. (2005). Direct activation of glucose transport in primary human myotubes after activation of peroxisome proliferator-activated receptor δ. Diabetes 54: 1157-1163.

Kubota T, Kubota N, Kumagai H, Yamaguchi S, Kozono H, Takahashi T *et al*. (2011). Impaired insulin signaling in endothelial cells reduces insulin-induced glucose uptake by skeletal muscle. Cell Metab 13: 294-307.

Lee CH, Olson P, Evans RM (2003). Minireview: lipid metabolism, metabolic diseases, and peroxisome proliferator-activated receptors. Endocrinology 144: 2201-2207.

Leibowitz MD, Fiévet C, Hennuyer N, Peinado-Onsurbe J, Duez H, Bergera J *et al*. (2000). Activation of PPARδ alters lipid metabolism in db/db mice. FEBS Lett 473: 333-336.

Lim HJ, Lee S, Park JH, Lee KS, Choi HE, Chung KS *et al.* (2009). PPAR delta agonist L-165041 inhibits rat vascular smooth muscle cell proliferation and migration via inhibition of cell cycle. Atherosclerosis 202: 446-454.

Lv ZM, Liu Y, Zhang PJ, Xu J, Jia ZH, Wang R *et al*. (2012). The role of AMPKα in high-glucose-induced dysfunction of cultured rat mesangial cells. Ren Fail 34: 616-621.

Miyazaki Y, Mahankali A, Matsuda M, Mahankali S, Hardies J, Cusi K *et al*. (2002). Effect of pioglitazone on abdominal fat distribution and insulin sensitivity in type 2 diabetic patients. J Clin Endocrinol Metab 87: 2784-2791.

Muniyappa R, Quon MJ (2007). Insulin action and insulin resistance in vascular endothelium. Curr Opin Clin Nutr Metab Care 10: 523-530.

Nishikawa T, Edelstein D, Du XL, Yamagishi S, Matsumura T, Kaneda Y *et al*. (2000). Normalizing mitochondrial superoxide production blocks three pathways of hyperglycaemic damage. Nature 404: 787-790.

Oliver Jr WR, Shenk JL, Snaith MR, Russell CS, Plunket KD, Bodkin NL *et al*. (2001). A selective peroxisome proliferator-activated receptor δ agonist promotes reverse cholesterol transport. Proc Natl Acad Sci USA 98: 5306-5311.

Patel MS, Korotchkina LG (2006). Regulation of the pyruvate dehydrogenase complex. Biochem Soc Trans 34: 217-222.

Piqueras L, Sanz MJ, Perretti M, Morcillo E, Norling L, Mitchell JA *et al.* (2009). Activation of PPARbeta/delta inhibits leukocyte recruitment, cell adhesion molecule expression, and chemokine release. J Leukoc Biol 86: 115-122.

Quintela AM, Jiménez R, Gómez-Guzmán M, Zarzuelo MJ, Galindo P, Sánchez M *et al.* (20012). Activation of peroxisome proliferator-activated receptor-β/-δ (PPARβ/δ) prevents endothelial dysfunction in type 1 diabetic rats. Free Radic Biol Med 53: 730-741.

Rains JL, Jain SK (2011). Oxidative stress, insulin signaling, and diabetes. Free Radic Biol Med 50: 567-575.

Reilly SM, Lee CH (2008). PPAR delta as a therapeutic target in metabolic disease. FEBS Lett 582: 26-31.

Reznick RM, Shulman GI (2006). The role of AMP-activated protein kinase in mitochondrial biogenesis. J Physiol 574: 33-39.

Rodríguez-Calvo R, Serrano L, Coll T, Moullan N, Sánchez RM, Merlos M *et al*. (2008). Activation of peroxisome proliferator-activated receptor beta/delta inhibits lipopolysaccharide-induced cytokine production in adipocytes by lowering nuclear factor-kappaB activity via extracellular signal-related kinase 1/2. Diabetes 57: 2149-2157.

Salt IP, Morrow VA, Brandie FM, Connell JM, Petrie JR (2003). High glucose inhibits insulin-stimulated nitric oxide production without reducing endothelial nitric-oxide synthase Ser1177 phosphorylation in human aortic endothelial cells. J Biol Chem 278: 18791-18797.

Saltiel AR, Kahn CR (2001). Insulin signalling and the regulation of glucose and lipid metabolism. Nature 414: 799-806.

Schnyder B, Pittet M, Durand J, Schnyder-Candrian S (2002). Rapid effects of glucose on the insulin signaling of endothelial NO generation and epithelial Na transport. Am J Physiol Endocrinol Metab 282: E87-E94.

Serrano-Marco L, Rodríguez-Calvo R, El Kochairi I, Palomer X, Michalik L, Wahli W *et al*. (2011). Activation of peroxisome proliferator-activated receptor-β/-δ (PPAR-β/-δ) ameliorates insulin signaling and reduces SOCS3 levels by inhibiting STAT3 in interleukin-6-stimulated adipocytes. Diabetes 60: 1990-1999.

Taguchi A, White MF (2008). Insulin-like signaling, nutrient homeostasis, and life span. Annu Rev Physiol 70: 191-212.

Tanaka T, Yamamoto J, Iwasaki S, Asaba H, Hamura H, Ikeda Y *et al*. (2003). Activation of peroxisome proliferator-activated receptor δ induces fatty acid β-oxidation in skeletal muscle and attenuates metabolic syndrome. Proc Natl Acad Sci USA 100: 15924-15929

Terada S, Wicke S, Holloszy JO, Han DH (2006). PPARdelta activator GW-501516 has no acute effect on glucose transport in skeletal muscle. Am J Physiol Endocrinol Metab 290: E607-E611.

Thors B, Halldórsson H, Jónsdóttir G, Thorgeirsson G (2008). Mechanism of thrombin mediated eNOS phosphorylation in endothelial cells is dependent on ATP levels after stimulation. Biochim Biophys Acta 1783: 1893-1902.

Tian XY, Wong WT, Wang NP, Lu Y, Cheang WS, Liu J, *et al.* (2012). PPAR delta Activation Protects Endothelial Function in Diabetic Mice. Diabetes 61: 3285-3293.

Tonelli J, Li W, Kishore P, Pajvani UB, Kwon E, Weaver C *et al*. (2004). Mechanisms of early insulin-sensitizing effects of thiazolidinediones in type 2 diabetes. Diabetes 53: 1621-1629.

Vincent MA, Montagnani M, Quon MJ (2003). Molecular and physiologic actions of insulin related to production of nitric oxide in vascular endothelium. Curr Diab Rep 3: 279-288.

Wallis MG, Smith ME, Kolka CM, Zhang L, Richards SM, Rattigan S *et al.* (2005). Acute glucosamine-induced insulin resistance in muscle in vivo is associated with impaired capillary recruitment. Diabetologia 48: 2131-2139.

Wang YX, Lee CH, Tiep S, Yu RT, Ham J, Kang H *et al*. (2003). Peroxisome-proliferator-activated receptor delta activates fat metabolism to prevent obesity. Cell 113: 159-170.

White MF (2003). Insulin signaling in health and disease. Science 302: 1710-1711.

Winzell MS, Wulff EM, Olsen GS, Sauerberg P, Gotfredsen CF, Ahrén B (2010). Improved insulin sensitivity and islet function after PPARδ activation in diabetic db/db mice. Eur J Pharmacol 626: 297-305.

Xu B, Chibber R, Ruggiero D, Kohner E, Ritter J, Ferro A (2003). Impairment of vascular endothelial nitric oxide synthase activity by advanced glycation end products. FASEB J 17: 1289-1291.

Zarzuelo MJ, Jiménez R, Galindo P, Sánchez M, Nieto A, Romero M *et al.* (2011). Antihypertensive effects of peroxisome proliferator-activated receptor-β activation in spontaneously hypertensive rats. Hypertension 58: 733-743.

FIGURE LEGENDS

Figure 1

Impaired insulin signaling in HUVECs exposed to high glucose. NO released from HUVECs incubated during 24 hours in low (LG, 5 mmol/L) or high glucose (HG, 30 mmol/L) medium was measured by DAF-2 fluorescence. Insulin (500 nmol/L) (A) or the calcium ionophore calimycin (A23187, 1 μmol/L) (B) were added at time 0. Results are mean ± SEM (n = 8) and $^{*}P < 0.05$, $^{**}P < 0.01$ *vs* cells exposed to low glucose. Expression of phospho-Akt (C) and phospho-eNOS (D) by Western blot in HUVECs in 5 or 30 mmol/L glucose, under basal and insulin (500 nmol/L for 10 min) stimulated conditions. Results are means ± SEM (n = 4–6) of densitometric values normalized to the corresponding Akt or eNOS. $^{*}P < 0.05$ *vs* low glucose and $^{\#\#}P< 0.01$ insulin *vs* basal.

Figure 2

Effects of PPAR-β agonists on impaired insulin signaling in high glucose medium. Insulin-mediated NO production in HUVECs exposed to low (5 mmol/L, A and B) or high (30 mmol/L, C and D) glucose medium for 24 hours coincubated with or without the PPAR-β agonists, L165041 (L, 1 and 10 μmol/L) (A and C) or GW0742 (GW, 1 and 10 μmol/L) (B and D). Experiments were also performed in HUVECs co-incubated with the PPAR-β antagonist GSK0660 (GSK, 1 μmol/L). Akt (E) and eNOS (F) phosphorylation was measured in HUVECs exposed to high glucose medium for 24 hours coincubated with or without the PPAR-β agonists (10 μmol/L) and then with insulin for 10 min. All data are mean ± SEM (n = 8). Data presented as densitometric values protein band normalized to the corresponding Akt or to the corresponding eNOS.

Panel show representative bands (n = 4–6). $^{*}P < 0.05$ and $^{**}P < 0.01$ *vs* control condition. $^{\#}P < 0.05$ and $^{\#\#}P < 0.01$ *vs* without GSK conditions.

Figure 3

siRNA knockdown of PPAR-β abolishes the effects of the PPAR-β agonists. Expression of PPAR-β at the level of mRNA expression by real time RT-PCR (A) and protein by western blot (B) in HUVECs transfected with either PPAR-β-specific siRNA (siRNA-PPAR-β) or empty vector (siRNA-control). Data are presented as gene expression normalized to GAPDH levels or densitometric protein band and normalized to the corresponding β-actin. Results are representative of n = 4 independent experiments. $^{*}P < 0.05$ *vs* siRNA-control. Insulin-mediated NO production (C) in control siRNA and siRNA-PPAR-β cells incubated in low (LG, □) or high glucose (HG, ■) medium for 24 h, in the presence or absence of GW0742 or L165041 (10 μmol/L) alone or preincubated with GSK0660 (1 μmol/L). All data are mean ± SEM (n = 8). $^{**}P < 0.01$ *vs* low glucose medium. $^{\#}P < 0.05$ and $^{\#\#}P < 0.01$*vs* without PPAR agonist in high glucose medium. $^{\dagger}P < 0.05$, vs L or GW column.

Figure 4

Role of the PPAR-β target genes, CPT-1 and PDK4 in the protective effects of PPAR-β agonists. Insulin-mediated NO production (A) and mRNA expression of PDK4 by real time RT-PCR (B, C) in HUVECs exposed to low (5 mmol/L, LG) or high glucose (30 mmol/L, HG) medium for 24 hours with or without the PPAR-β agonists, L165041 or GW0742 (10 μmol/L) alone or preincubated with an irreversible inhibitor of CPT-1, etomoxir (40 μmol/L) or an inhibitor of PDK4, DCA (10 μmol/L) 30 min before measuring the insulin-mediated NO production at 15 min. (D) Left, expression of

PDK4 protein by western blot in HUVECs transfected with either PDK4-specific siRNA (siRNA-PDK4) or empty vector (siRNA-control). Data are presented as densitometric protein band and normalized to the corresponding β-actin. Results are representative of n = 4 independent experiments. **P < 0.01 vs siRNA-control. Right, insulin-mediated NO production in control siRNA and siRNA-PDK4 cells incubated in low (LG) or high glucose (HG) medium for 24 h, in the presence or absence of GW0742 or L165041 (10 μmol/L). All data are mean ± SEM (n = 8). mRNA data presented as a ratio of arbitrary units of mRNA ($2^{-\Delta\Delta Ct}$). $^{*}P < 0.05$ and $^{**}P < 0.01$ *vs* control condition, $^{\#\#}P < 0.01$ *vs* L and GW column, respectively.

Figure 5

Effects of the PPAR-β agonists in intracellular ROS production. CM-H_2DCFDA-detected intracellular ROS in HUVECs (A) and HUVEC transfected with PPAR-β-specific siRNA (siRNA-PPAR-β) (B), or with PDK4-specific siRNA (siRNA-PDK4) (C) incubated in low (5 mmol/L, LG) or high glucose (30 mmol/L, HG) medium for 24 hours in the presence or absence of either L165041 (1μmol/L), or the inhibitor of complex I rotenone (5 μmol/L), or the inhibitor of complex II, thenoyltrifluoroacetone (TTFA 10 μmol/L), or the uncoupler of oxidative phosphorylation, carbonyl cyanide m-chlorophenylhydrazone (CCCP, 0.5 μmol/L). Inhibitors (GSK0660 1μmol/L, DCA 10 μmol/L, or MitoQ 0.1 μmol/L) were added 30 (GSK0660, or DCA) or 60 (MitoQ) min before the incubation with L165041. (D) mRNA expression of MnSOD by real time RT-PCR in HUVECs exposed to low (5 mmol/L, LG) or high glucose (30 mmol/L, HG) medium for 24 hours with or without the PPAR-β agonists, L165041 or GW0742 (10 μmol/L) alone or co-incubated with the PPAR-β antagonist GSK0660 (GSK, 1 μmol/L). (E) ERK1/2 phosphorylation in HUVECs incubated in the presence of TTFA and

catalase. Data represent the mean ± SEM (n = 8), and the experiments were repeated independently at least three times. Data presented as densitometric values protein band normalized to the corresponding ERK 1/2. Panel shows representative bands (n = 3-5). $^{*}P < 0.05$ and $^{**}P < 0.01$ *vs* low glucose medium, respectively. $^{\#}P < 0.05$ and $^{\#\#}P < 0.01$ *vs* high glucose medium.$^{\dagger}P < 0.05$ *vs* L or GW column without inhibitor.

Figure 6

Effects of PPAR-β agonists on IRS phosphorylation. Ser-636-IRS-1 (A) or Ser-270-IRS-1/2 (B) phosphorylation by Western blot in HUVECs incubated in low (5 mmol/L, LG) or high glucose (30 mmol/L, HG) medium for 24 hours with or without the PPAR-β agonists, L165041 (L, 10 μmol/L) or GW0742 (GW, 10 μmol/L), alone or preincubated with the PPAR-β antagonist GSK0660 (1 μmol/L) or the ERK1/2 inhibitor, PD98059 (10 μmol/L). Data presented as densitometric values protein band normalized to the corresponding α-actin. Panel shows representative bands (n = 3-5). $^{**}P < 0.01$ *vs* low glucose medium. $^{\#\#}P < 0.01$ *vs* drug free in high glucose medium. $^{\dagger}P < 0.05$ *vs* L and GW column, respectively.

Figure 7

GW0742 treatment *in vivo* restored NO-mediated relaxation induced by insulin in vessels from streptozotocin (STZ)-induced diabetic rats. GW0742 (5 mg/kg/day for 3 days) treatment was started 4 days after STZ injection. Plasma glucose levels (A), and mRNA aortic expression of PDK4 and MnSOD by real time RT-PCR (B). Phosphorylation of eNOS and Akt induced by insulin (100 nM) in aorta (C). Relaxation induced by insulin in aorta (D) and in mesenteric arteries (E) precontracted by phenylephrine (Phe, 1 μmol/L), in the absence or presence of the PDK-4 inhibitor

(DCA, 10 μmol/L), or the mitochondrial antioxidant mitoQ (0.1 μmol/L) for 1 h before Phe. All data are mean ± SEM (n = 10). $^{*}P < 0.05$ and $^{**}P < 0.01$ *vs* control (non diabetic rats treated with vehicle) group, $^{\#}P < 0.05$ and $^{\#\#}P < 0.01$ *vs* STZ, respectively.

Figure 8

Scheme representing the insulin signaling pathway, the mechanisms involved in the high glucose-induced impairment of the insulin pathway and the proposed mechanism by which PPAR-β agonists prevent high glucose-induced insulin resistance in HUVECs.

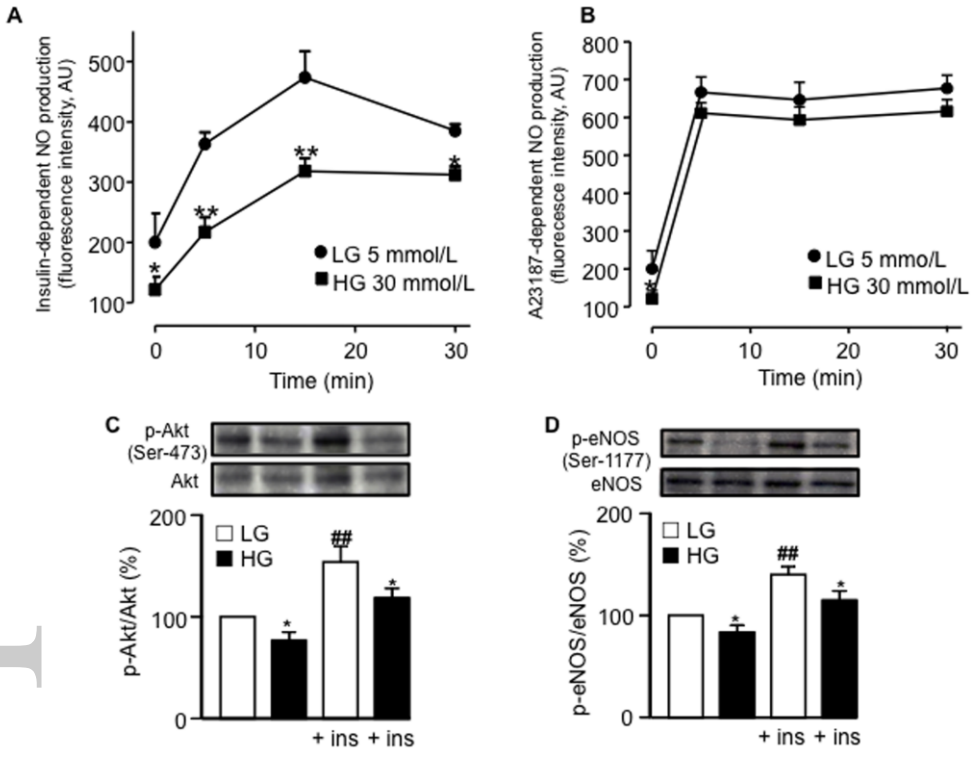

Figure 1

bph_12646_f1

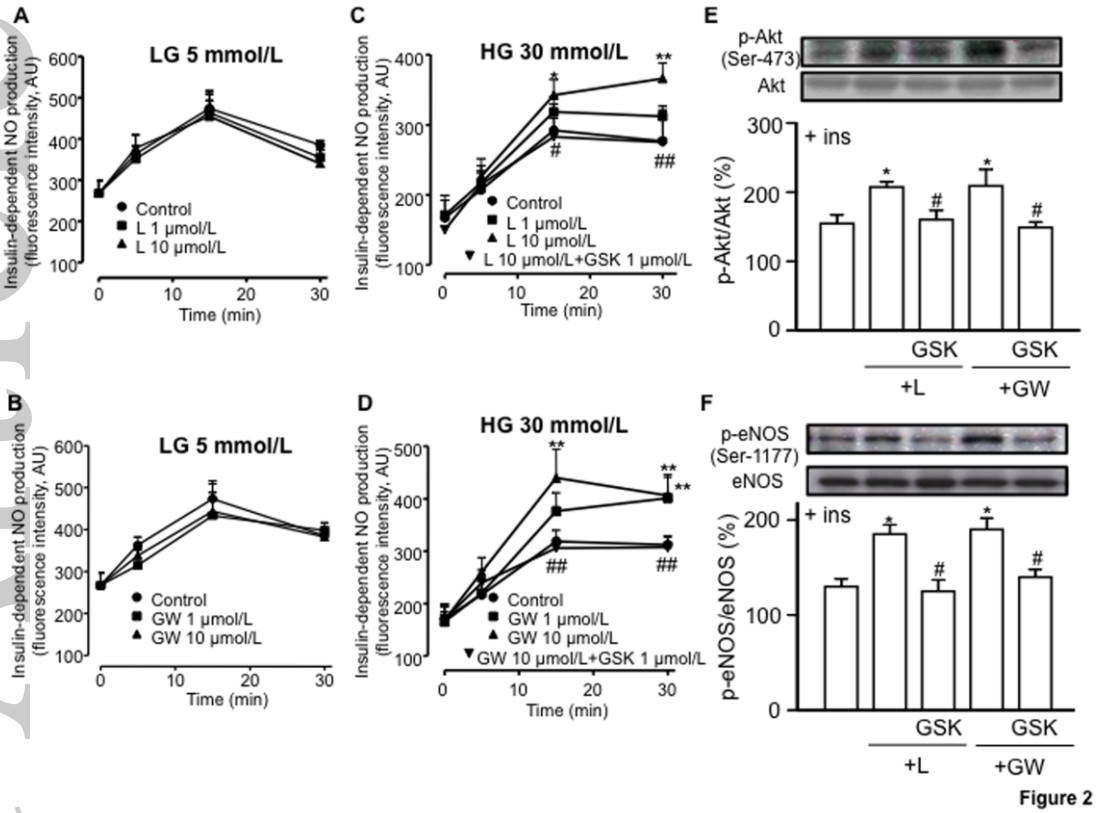

Figure 2

bph_12646_f2

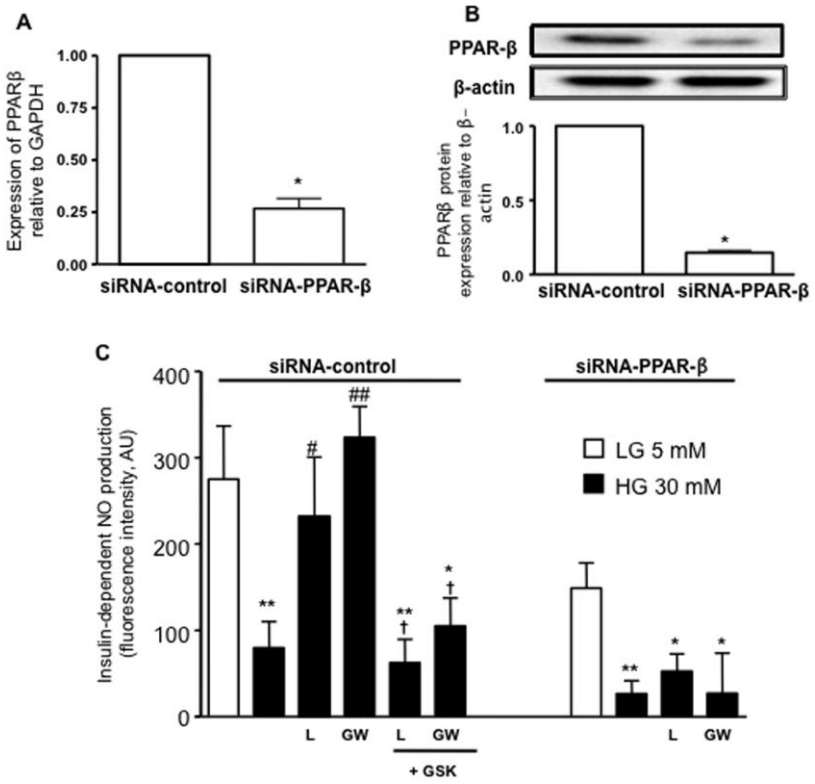

Figure 3

bph_12646_f3

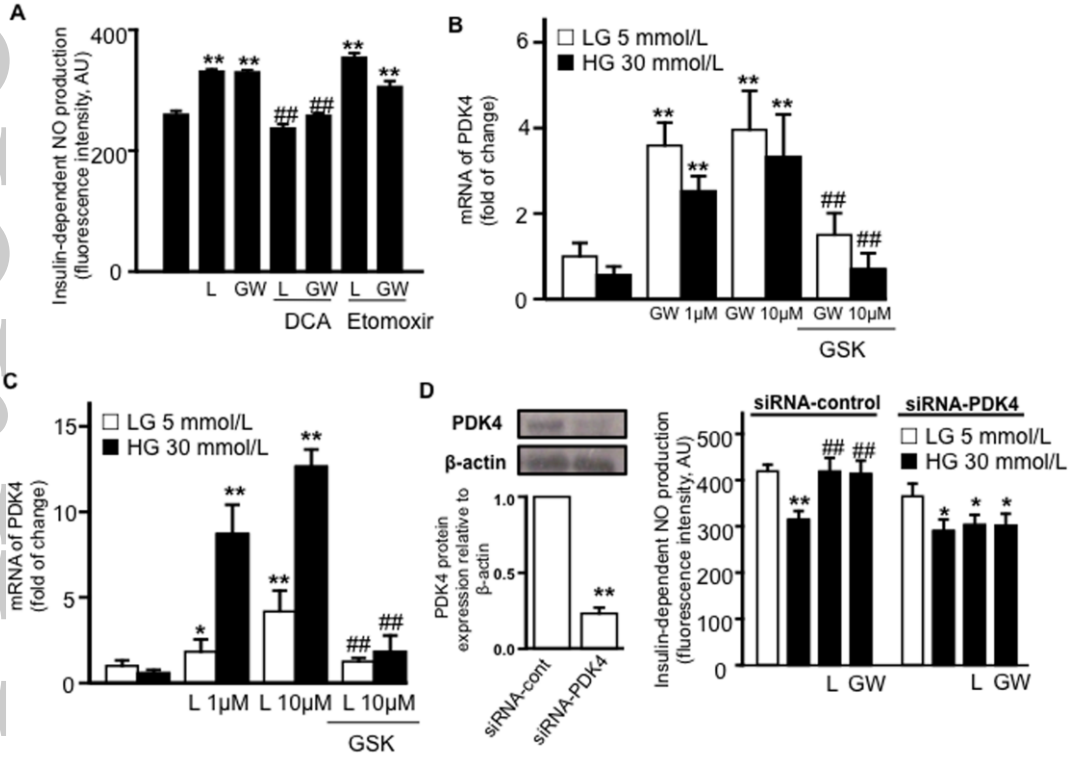

Figure 4

bph_12646_f4

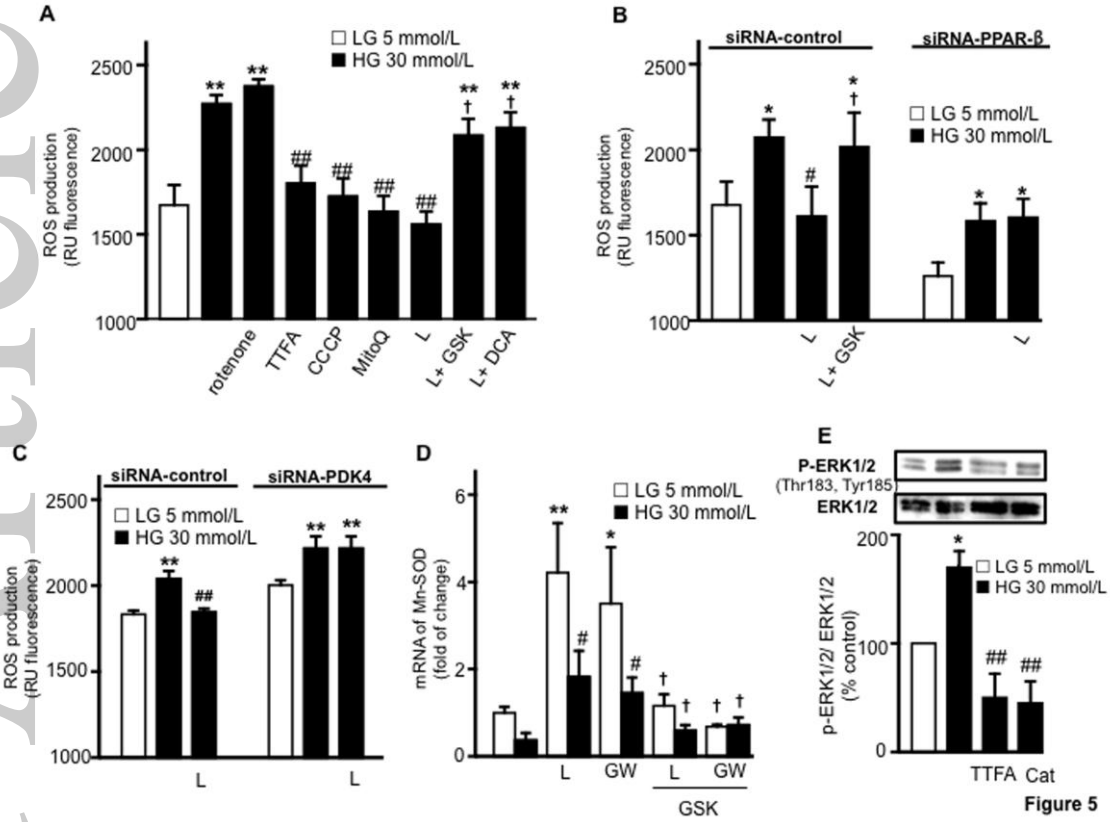

Figure 5

bph_12646_f5

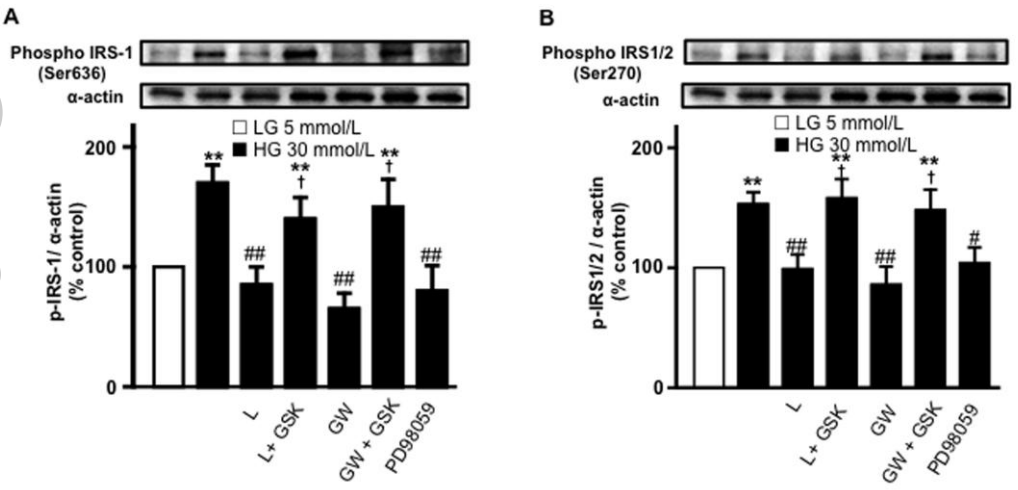

Figure 6

bph_12646_f6

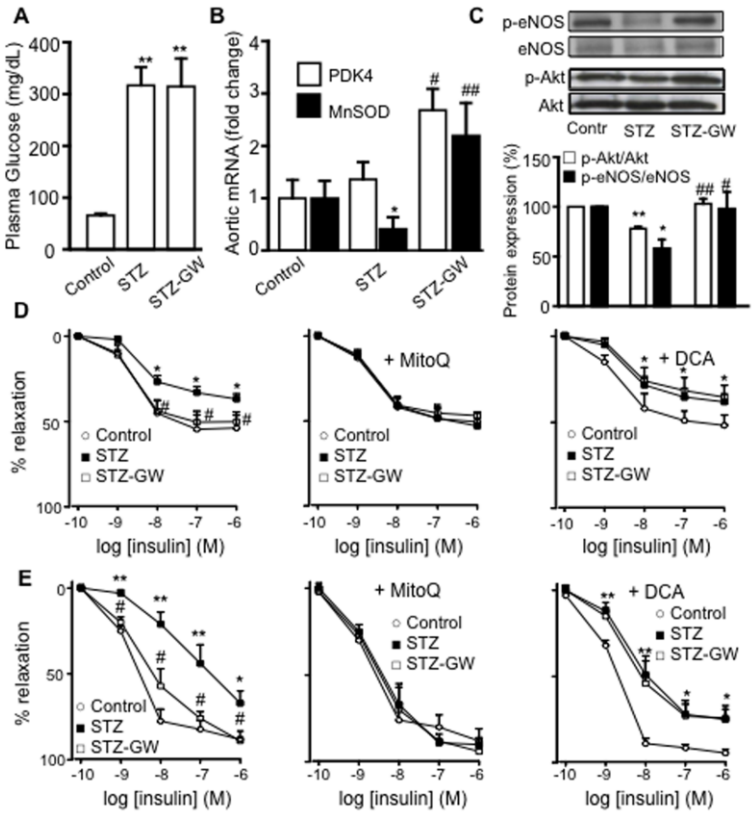

Figure 7

bph_12646_f7

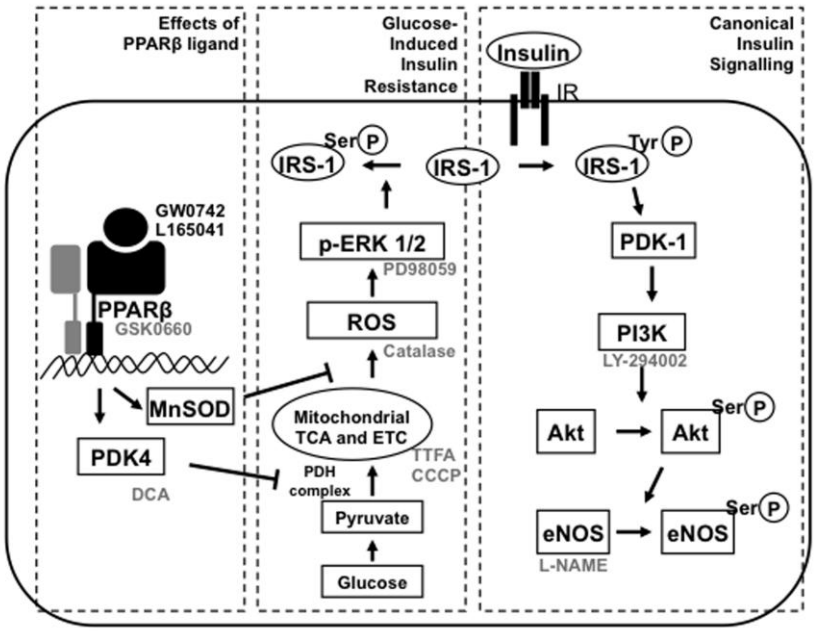

Figure 8

bph_12646_f8